The final version of this manuscript appeared in the proceedings of the IEEE MoNaCom 2013 workshop, 9-13 June 2013, Budapest, Hungary.

Introducing purely hydrodynamic networking mechanisms in microfluidic systems

Andrea Biral, Andrea Zanella

***Abstract*—Microfluidic is a multidisciplinary field with practical applications to the design of systems, called Lab-on-a-Chip (LoC), where tiny volumes of fluids are circulated through channels with millimeter size and driven into structures where precise chemical/physical processes take place. One subcategory of microfluidic is droplet-based microfluidic, which disperse discrete volumes of fluids into a continuous stream of another immiscible fluid, which act as droplet carrier. Droplets can then be moved, merged, split, or processed in many other ways by suitably managing the hydrodynamic parameters of the LoC. A very interesting research challenge consists in developing basic microfluidic structures able to interconnect specialized LoCs by means of a flexible and modular microfluidic network. The aim of this paper is to exploit the properties of droplet-based microfluidics to realize purely hydrodynamic microfluidic elements that provide basic networking functionalities, such as addressing and switching. We define some simple mathematical models that capture the macroscopic behavior of droplets in microfluidic networks and use such models to design and analyze a simple microfluidic network system with bus topology.**

***Index Terms*—Microfluidics, droplet, switching, network, lab-on-a-chip, purely hydrodynamic switching**

I. Introduction

When fluids are constrained in channels with sumbillimeter diameters (from hundreds of nanometers to hundreds of micrometers), the Reynolds number, which accounts for the impact of fluid's momentum to viscosity, can become very low and fluids may exhibit specific behaviors that are unobserved at "normal" scales. For instance, fluids that are normally mixable, when constrained in micro channels may flow in parallel streams, without mixing [1]. These properties are at the basis of a number of applications, ranging from the inkjet printer heads to DNA chips, and have been recently exploited in the development of Lab-on-Chip (LoC) systems, which are used to perform precise chemical/physical processes with very limited amount of reactants.

The analysis and control of fluid dynamics at very low Reynolds number is the subject of the multidisciplinary science known as *microfluidic*. A branch of microfluidic focuses on droplet-base systems, where discrete volumes of fluids are dispersed into a continuous stream of another immiscible fluid that acts as droplet carrier. Droplets can then be moved, merged, split, or processed in many ways by suitably managing the hydrodynamic parameters of the LoC [2]. The advantages offered by the microfluidics technology are numerous and various, in particular in the chemical and pharmaceutical industry, where LoCs are currently used for different purposes, included the synthesis of particles for therapeutic delivery, drug discovery, biomolecule synthesis, diagnostic testing, DNA sequencing.

Today, however, most LoC systems are highly specialized and can perform only an extremely limited set of specific operations, in a predefined order. An emerging research trend aims at enhancing the potential of this technology by introducing devices and methods to interconnect different LoCs in a flexible system [3]. The specificities of the microfluidics, however, require a deep revision of the traditional networking approaches while opening the way to a plethora of novel research challenges.

Droplets can be manipulated with high precision, by means of electro-hydrodynamics (EHD) stresses that, however, require complex and costly micro-fabrication of arrays of independently addressable electrodes [5]. Conversely, pure hydrodynamic droplet manipulation does not require in-chip electronics and only relies on the actuators (pumps and reservoirs) at the edge of the chip. These features make purely hydrodynamic solutions very attractive for specific application domains (e.g., body implants).

The related basic working principle is that droplets flow along the path with minimum instantaneous fluidic resistance, meanwhile increasing the resistance of the channel. Then, an isolated droplet entering a T or Y junction through the inlet will proceed toward the outlet with minimum instantaneous fluidic resistance [6]. However, the fluidic resistance of that branch is temporarily increased by the presence of the droplet, so that successive droplets may be driven to the other outlet. It is hence possible to steer a *payload* droplet through a series of junctions by modulating its distance with respect to a certain number of *control* droplets [7]. Furthermore, recent discoveries have demonstrated that droplet microfluidic systems can perform basic Boolean logic functions, such as AND, OR and NOT gates, and bistable devices [8]. These studies pave the way to the realization of microfluidic computing and switching elements that are the basis of microfluidic networks [4].

In this paper we wish to advance the first steps along this road by demonstrating that complex networking functions can be introduced in LoC context by using only microfluidic devices based on hydrodynamic principles. To this end, we propose simplified mathematical models that provide a high-level description of some specific actions, such as droplet formation, transport and splitting, fluidic resistance control, and switching. These models are first validated by means of low-level simulations performed with the OpenFOAM[1]

The authors are with the Department of Information Engineering, University of Padova, Via G. Gradenigo 6/B, 35131 Padova, Italy. Office: +39 049 827 7770, fax: +39 049 827 7699, mailto: zanella@dei.unipd.it

[1]http://www.openfoam.com

software package, which keeps into accounts the details of the fluid dynamics. We then apply these models to the design and performance analysis of a simple microfluidic network with bus topology.

II. Modeling of basic microfluidic features

A droplet-based microfluidic network consists of a network of micro-channels, with possibly different sizes and shapes, which are filled by a carrier fluid, called *continuous phase*. The fluid is injected into the channels by external pumps, such as syringe and peristaltic pumps, that can regulate the volumetric flow rate Q $[m^3/s]$ or the pressure drop ΔP $[Pa]$ of the continuous phase in the channel. The continuous phase can carry droplets of another fluid, called *dispersed phase*, which are injected into the continuous flow by other pumps. When arriving to a junction, a droplet will follow the branch with instantaneous lower fluidic resistance that, for a microchannel with rectangular section, can be expressed as

$$R(\mu, L) = \frac{a\mu L}{wh^3}\,, \tag{1}$$

where L, w, h are length, width and height of the channel ([meter]), μ is the dynamic viscosity of the fluid ($[Pa\,s]$), whereas a is a dimensionless parameter defined as $a = 12[1 - \frac{192h}{\pi^5 w}\tanh(\frac{\pi w}{2h})]^{-1}$. The presence of a droplet in a channel, however, will increase the fluidic resistance of that channel, so that the actual fluidic resistance in the different parts of a microfluidic network may change over time, depending on the paths followed by the droplets, and on their size.

In the following, we analyze in more details these aspects, proposing some simplified mathematical models that are used to correctly dimensioning a droplet-based microfluidic network. For the sake of simplicity, we focus on channels with uniform rectangular section of size $w \times h$.

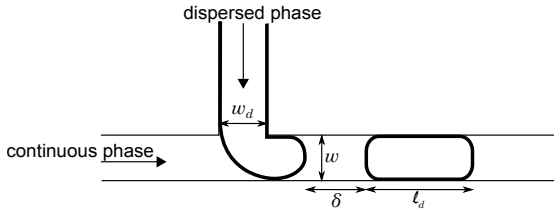

Fig. 1. Example of droplet production in a T-junction (top view).

A. Droplets generation

Droplets can be created by injecting the dispersed phase into the continuous phase through a T-junction [9], as shown in Fig. 1. The volumetric flow rates Q_c and Q_d of the continuous and dispersed fluids are commonly controlled via independent syringe pumps. The creation of droplet is governed by the *Capillary number*, C_a, a dimensionless parameter that describes the relative magnitude of the viscous shear stress compared with the interfacial tension, given by

$$C_a = \frac{\mu_c u_c}{\sigma} = \frac{\mu_c Q_c}{\sigma w h}. \tag{2}$$

where $u_c = \frac{Q_c}{wh}$ is the average velocity of the continuous stream, μ_c is its dynamic viscosity and σ $[N/m]$ is the interfacial tension coefficient between dispersed and continuous phase. Droplets' shape is highly controllable only in the so-called *squeezing regime* [10], [11], which requires

$$C_a < C_a^* \approx 10^{-2}\,. \tag{3}$$

The length ℓ_d of the droplets created at the T-junction in the squeezing regime can be approximated as

$$\ell_d = w\left(1 + \alpha\frac{Q_d}{Qc}\right)\,, \tag{4}$$

where α is a dimensionless parameter of order one [11]. The droplet length can then be tuned by playing with the volumetric flow rates Q_c and Q_d, provided that the constraint (3) on the capillary number holds.

From (4), applying a simple mass conservation argument, we can determine the approximate expression of the inter-droplet distance

$$\delta = \frac{Q_c}{Q_d}\ell_d = \frac{Q_c}{Q_d}w\left(1 + \alpha\frac{Q_d}{Qc}\right). \tag{5}$$

Note that ℓ_d and δ are determined by the same set of parameters, so that they are jointly settled.

We corroborated the analytical models by means of OpenFOAM's simulations, which confirmed the validity of condition (3) and of formulae (4) and (5). However, we observed that setting Q_d/Q_c beyond a certain threshold (equal to 7 in our simulations), the squeezing regime degenerates and anomalous behaviors emerge, despite condition (3) holds. Therefore, to be reasonably sure that the system works in the squeezing regime, the length of the droplets generated with this technique shall be significantly less than $w(1 + 7\alpha)$.

B. Droplets' effect on fluidic resistance

When a droplet is injected into a duct, the friction generated with the carrier fluid and the forces produced by the inhomogeneity between the dynamic viscosity of continuous and dispersed phases determine an increase of the fluidic resistance of the channel [12], [13], [14]. For our purposes, we need to define a simple model to approximate the resistance's variation produced by a droplet in a microchannel. To this end, we consider the case exemplified in Fig. 1, where a droplet with dynamic viscosity μ_d occupies a segment of length ℓ_d of the channel, otherwise filled by the continuous phase with dynamic viscosity μ_c. According to (1), the fluidic resistance of a channel of length L without droplets is $R = R(\mu_c, L)$. The variation of resistance produced by a droplet of length ℓ_d injected into such a channel can then be approximated as

$$\rho(\ell_d) = R(\mu_c, L-\ell_d) + R(\mu_d, \ell_d) - R = (\mu_d - \mu_c)\frac{\ell_d a}{wh^3}\,. \tag{6}$$

Note that, according to our model, the presence of a droplet increases the hydraulic resistance of the channel only if $\mu_d > \mu_c$, whereas in the contrary case, the resistance is actually decreased by the droplet. An intuitive explanation is that the greater the viscosity ratio $\lambda = \mu_d/\mu_c$, the greater the resistance of the droplet to flow. This behavior is consistent with the

outcome of OpenFOAM simulations, though it is in contrast with some experimental results where it was observed an increase of the channel resistance even with $\lambda < 1$. A possible explanation for such inconsistency is that neither our model, nor the OpenFOAM simulator take into account friction's sources different from viscous force (e.g., the pressure exerted to the droplet by the thin films of continuous phase that wrap the dispersed fluid). Consequently, the proposed model may fail when viscous forces are not the dominant friction contribution and, hence, it is mainly applicable when $\lambda \gg 1$.

C. Junction crossing

A typical microfluidic junction consists of a channel that forks into two branches, usually in T or Y shape. The pattern followed by droplets across a junction may either be regular or chaotic, depending on a number of factors. Furthermore, droplets may collide, coalesce or split when crossing a junction, as observed in several studies [12], [13], [14], [15].

Focusing on T-junctions, a droplet can either split into the two outgoing branches (*breakup regime*) or stay compact and flow along the branch with minimum instantaneous fluidic resistance (*non-breakup regime*). According to the mathematical model proposed in [14], the non-breakup regime is observed when

$$\ell_d < \ell_d^* \approx \chi w C_a^{-0.21} \tag{7}$$

where χ is a dimensionless parameter that decreases as the viscosity ratio λ increases [16]. Although derived for the 2D case, the boundary condition (7) suitably agrees with our 3D simulations and other experimental results [17].

D. Switching principle

As mentioned, in the non-breakup regime, a droplet entering the T-junction will steer to the outlet with least instantaneous fluidic resistance, say R_1 or, equivalently, maximum volumetric flow rate, Q_1. However, the presence of the droplet increases the resistance of the selected outlet by a factor ρ, as given by (6). If $R_1 + \rho$ is greater than the fluidic resistance R_2 of the other outgoing branch, a second droplet closely following the first one will be steered on the second outlet. This phenomenon can be exploited to design simple droplet-switching mechanisms, where a cargo droplet can be preceded by one or more control droplets that modify the instantaneous flow rates seen by the cargo in order to steer it in a controlled fashion to the desired location. Borrowing from the ICT terminology, we use the terms *header* and *payload* to refer to the control and cargo droplets, respectively.

Playing with the length of the outlets in T-junction and the length of the header droplet, it is possible to control the path followed by the payload droplet through a number of serial switches, as it will better explained later on in this paper.

III. Microfluidic-electronic duality

As seen, the behavior of microfluidic systems is affected by a number of interdependent factors that make the fluids flow at any one location dependent on the properties of the entire system. However, the models defined in the previous section provide an abstraction of some fundamental microfluidic mechanisms that, while concealing the details of the underlying physical phenomena, captures the "macroscopic" aspects concerning the design of a more complex systems. The analysis can be further simplified by exploiting the parallel between continuous-flow microfluidic systems and electric circuits, as observed in some recent literature [18], [19].

According to this duality principle, the pressure difference ΔP, volumetric flow rate Q, and hydraulic resistance R of a microfluidic channel can be associated to the voltage drop ΔV, current intensity I, and ohmic resistance R_E of an electric line. Correspondingly, Ohm's and Kirkhhoff's current and voltage laws,

$$\Delta V = R_E I\,, \quad \sum_{m=1}^{M} I_m = 0\,; \quad \sum_{k=1}^{K} V_k = 0\,; \tag{8}$$

find their counterparts in the Hagen-Poiseuille's law, and the flow and energy conservation laws in microfluidics circuits:

$$\Delta P = RQ\,, \quad \sum_{m=1}^{M} Q_m = 0\,, \quad \sum_{k=1}^{K} \Delta P_k = 0\,, \tag{9}$$

where M is the number of branches emanating from a junction, while K is the number of continuous channel segments in a generic closed loop. As a consequence, the equivalent hydraulic resistance of a series of H microfluidic resistors is the sum of all H resistances, while the conductance of the parallel of H resistors is the sum of their conductances. The analogy between electric and microfluidic circuits can be further extended to voltage/current sources and external pumps, such as syringe and peristaltic pumps, used to supply constant pressure/fluid flow, as illustrated in Fig. 2.

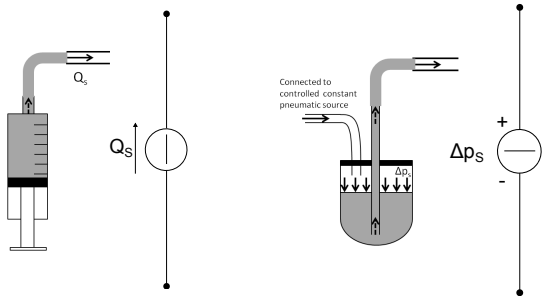

Fig. 2. Analogy between constant fluidic flow source and current generator (left), constant fluidic pressure source and voltage generator (right).

IV. Case study: bus-topology

As a proof of concept, we apply the theory presented in the previous sections to the design of a simple purely hydrodynamic microfluidic network, with the bus topology sketched in the upper part of Fig. 3. More specifically, the system consists of a main channel (the *bus*) with N secondary channels, which are perpendicularly grafted into the bus at regular distance L, thus forming a series of N consecutive T-junctions that lead to N different microfluidic machines or LoCs. The continuous phase is pumped with constant flow rate from the leftmost end of the bus and completely fills up the bus and all the outlets, exiting the circuit from the rightmost

end of the bus, and from the N LoCs. Outlets leading to the LoCs are numbered from 1 to N, starting from the end of the bus and moving upstream towards the source. The length of the nth branch is denoted by L_n and, as it will be explained shortly, it increases with n.

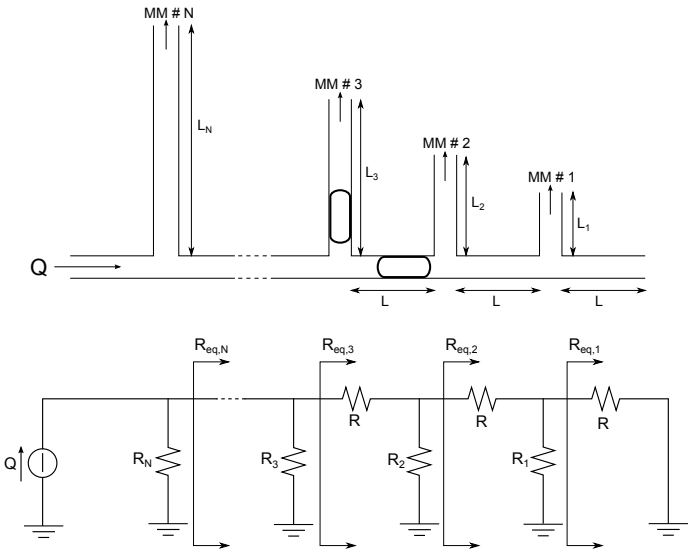

Fig. 3. Microfluidic network with bus topology (upper) and corresponding electric circuit (lower).

The lower part of Fig. 3 depicts the electric circuit equivalent of the microfluidic bus network, as for the duality principle discussed in Sec. III. According to (1), the fluidic resistance of the nth outlet is given by $R_n = R(\mu_c, L_n)$, whereas the resistance of microfliduic segments that separate two consecutive outlets are all equal to $R = R(\mu_c, L)$. (Note that, in general, the resistance of the channels may also depend on the terminal LoCs, so that the expressions of R_n and R shall be adjusted accordingly.) As indicated in Fig. 3, the equivalent downstream electric/microfluidic resistance seen after each junction n can be recursively expressed as $R_{eq,1} = R$ and

$$R_{eq,n} = R + \frac{R_{n-1}R_{eq,n-1}}{R_{n-1} + R_{eq,n-1}}\,, \quad n = 2, \ldots, N \tag{10}$$

Such resistances are designed to achieve the desired behavior of the droplets. To begin with, in plain conditions, the leading stream shall always be along the bus, so that isolated droplets never steer on secondary channels. This requires that $R_n > R_{eq,n}$ for all $n = 1, \ldots, N$. To guarantee this condition, we set

$$R_n = \alpha R_{eq,n}\,, \tag{11}$$

where $\alpha > 1$ is a design parameter, whose role will be analyzed later on in this paper. Now, replacing (11) into (10) we get

$$R_n = \alpha R + R_{n-1}\frac{\alpha}{1+\alpha} \tag{12}$$

that, solving the recursion, yields

$$R_n = R\alpha(1+\alpha)\left(1 - \left(\frac{\alpha}{1+\alpha}\right)^n\right). \tag{13}$$

From (13) we see that, for any $n = 1, \ldots, N-1$, it holds

$$R_n < R_{n+1}\,, \quad \text{and} \quad R_{eq,n} < R_{eq,n+1} \tag{14}$$

according to which the lengths $\{L_n\}$ of the secondary branches increase with n, as depicted in Fig. 3.

Let ρ_n denote the resistance increase that shall be produced by a header droplet to steer a closely following payload droplet into the nth outlet. To this end, for each $n = 1, \ldots, N$ it shall hold

$$R_n - R_{eq,n} < \rho_n < \min\left\{R_j - R_{eq,j};\, j = n+1, \ldots, N\right\} \tag{15}$$

where we conventionally set $R_{N+1} - R_{eq,N+1} = \infty$. The right inequality guarantees that the payload droplet flows along the bus till it reaches the nth junction, while the left inequality assures the droplet takes the nth outbound branch. It is easy to realize that ρ_n can then take values in the interval

$$\Delta_n = (R_n - R_{eq,n}, R_{n+1} - R_{eq,n+1})\,, \quad n = 1, \ldots, N\,. \tag{16}$$

Using (11) in (16) we obtain

$$\Delta_n = \frac{\alpha - 1}{\alpha}(R_n, R_{n+1})\,, \quad n = 1, \ldots, N\,, \tag{17}$$

so that ρ_n can be expressed as

$$\begin{aligned}\rho_n &= \frac{\alpha-1}{\alpha}\left(\beta R_{n+1} + (1-\beta)R_n\right)\,, \\ &= R(\alpha^2-1)\left[1 - \left(\frac{\alpha}{1+\alpha}\right)^n\left(1 - \frac{\beta}{1+\alpha}\right)\right]\end{aligned} \tag{18}$$

where $\beta \in (0,1)$ is another design parameter. The range of admissible values for ρ_n is thus

$$|\Delta_n| = \frac{\alpha-1}{\alpha}(R_{n+1} - R_n) = RC_1(\alpha, n) \tag{19}$$

where the last step follows from (13), with

$$C_1(\alpha, n) = \frac{(\alpha-1)\alpha^n}{(\alpha+1)^n}\,. \tag{20}$$

The parameter $C_1(\alpha, n)$ is a measure of the design space of ρ_n: the smaller $C_1(\alpha, n)$, the stricter the interval of admissible values for ρ_n and, hence, the less robust the system to structural imperfections or process noise. For a given $\alpha > 1$, $C_1(\alpha, n)$ is monotonically decreasing in n and, for $n = N$, it reaches the minimum $C_1(\alpha, N) = (\alpha-1)[\alpha/(\alpha+1)]^N$. On the one hand, $C_1(\alpha, N)$ shall be as large as possible to increase system robustness. On the other hand, increasing $C_1(\alpha, N)$ requires larger α and, in turn, longer channels and higher resistances. Therefore, there is clearly a tradeoff between system robustness and efficiency.

Another constraint to the design parameter α is obtained by considering that the header droplets must be fully contained in the segment of length L that separates two consecutive outlets, otherwise the behavior at the junctions would not be longer predictable. As for (6), given the microfluidic channels geometry and the characteristics of the continuous and dispersed fluids, ρ_n is proportional to the length ℓ_n of the droplet dispersed in the channel, so that the maximum length of a header droplet will be ℓ_N. Therefore, we shall guarantee

$$\ell_N < L \tag{21}$$

that, using (1) and (6), can be expressed as

$$\rho_n < R(\lambda - 1) \tag{22}$$

where $\lambda = \mu_d/\mu_c$. Replacing (18) into (22) we finally get

$$C_2(\alpha, N) < 1 \tag{23}$$

where, for shortness of notation, we set

$$C_2(\alpha, N) = \frac{\alpha^2 - 1}{\lambda - 1}\left[1 - \left(\frac{\alpha}{1+\alpha}\right)^N \left(1 - \frac{\beta}{1+\alpha}\right)\right]. \tag{24}$$

Given β, condition (23) sets an upper bound to the admissible range of values that can be assigned to the design parameter α: the larger N, the lower the upper bound.

To guarantee a certain robustness of the network to the tolerances in the manufacturing and managing processes, we shall hence require

$$C_1(\alpha, N) > t_1\,, \quad C_2(\alpha, N) < t_2\,, \tag{25}$$

where the thresholds $t_1 > 0$ and $t_2 < 1$ are two design parameters. Intersecting the admissible regions defined by (25) we get the areas delimited by the curves in Fig. 4. Note that,

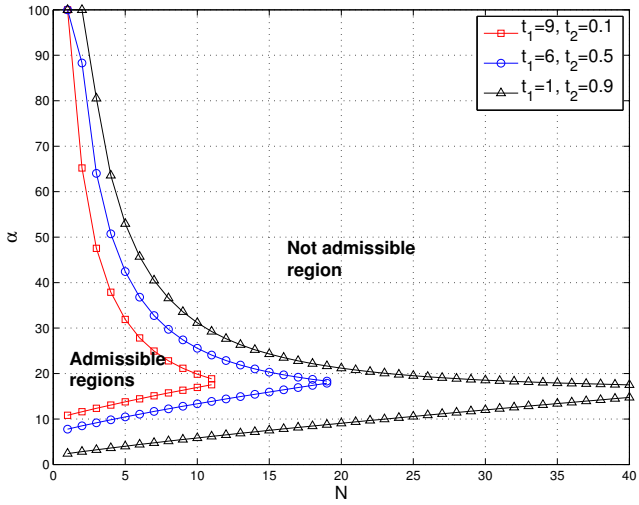

Fig. 4. Admissible range of α imposed by (25) as a function of N for various thresholds t_1, t_2 and $\beta = 0.5$.

given the thresholds t_1 and t_2, and $\beta = 0.5$, the borders of the admissible region intersect in correspondence of a certain N, denoted by N^*, which represents the maximum number of LoCs that can be connected into the bus network.

A. Performance analysis

Interconnecting different LoCs through purely hydrodynamic micrfluidic networks can potentially bring a number of advantages in terms of device flexibility, manufacturing costs, number and complexity of enabled analysis processes, and so on. From a networking perspective, some performance figures of interest are the number of supported LoCs, the mean time to carry a payload droplet to the intended LoC, the average number of payload droplets delivered in a unit time, the probability of "errors" (which include droplets coalescence, merging or splitting, wrong turn at junctions, and so on), the overhead, which can be intended as the cost of producing header droplets to control the payload droplets, and others.

In this work we focus on the *throughput* performance metric that, in the ICT domain, is generally defined as the mean number of information bits delivered to the intended destination in the unit time, and in the microfluidic context can be reinterpreted as the mean *volume* of payload droplets delivered to the intended LoC in the unit time, i.e.,

$$S = \lim_{t\to\infty} \frac{V(t)}{t} \tag{26}$$

where $V(t)$ is the total volume of dispersed fluid delivered to the intended receivers in time t.

The throughput depends on a number of factors, related to the physical parameters (kind of fluids, geometry of the microfluidic channels), structural features (network topology, number of destination LoC), and traffic-related aspects (droplet generation pattern, medium access scheme, routing). Here we considered the bus network of Fig. 3, with a number N of terminal LoCs that varies from 1 to 5. We assume *saturated droplet source*, so that a new payload droplet is injected into the bus as soon as possible, according to the adopted access scheduling policy. Payload droplets have all fixed volume v, and are intended for any of the N terminal LoCs, with equal probability. Finally, at this stage of the work, we focus on the simple *exclusive access* policy, according to which a new pair of header-payload droplets can be generated only after the previous pair has exited the system. In this conditions, the average throughput can be obtained as

$$S = \frac{v}{B}\,, \quad \text{with} \quad B = \sum_{n=1}^{N} \frac{b_n}{N} \tag{27}$$

where b_n is the time taken for both payload and header droplets to leave the system through the nth LOC and the rightmost bus outlet, respectively.

The time taken by a droplet to cross a segment depends on the volumetric flow rate of the continuous phase through that segment that, in turn, is affected by the location of the droplets in the network. Using the electric circuit parallel discussed in Sec. III, given the position of the droplets in the circuit, it is possible to compute the instantaneous resistance of each branch and, thus, determine the "current" intensity in each network segment. Any time a droplet leaves a segment for another one, we need to recompute the current distribution in the circuit, according to the new branch resistances. The process is repeated until both droplets leave the system and a new header-payload droplet can be injected.

Note that the flow rate in each channel is clearly proportional to the input velocity u of the continuous phase in the network. Therefore, increasing u, we speed up the droplets along the circuits, thus increasing the throughput. Increasing u beyond a certain threshold, however, may bring the system in the breakup regime, thus resulting in droplets splitting at junctions. Considering the non-breakup condition (7), and replacing C_a with the expression in (2) we indeed get

$$u < u^* = \frac{\sigma}{\mu_c}\left(\frac{\chi w}{\ell_d^*}\right)^{\frac{1}{0.21}} \tag{28}$$

where u^* is the maximum allowed input rate of the system to work in the non-breakup regime.

Summing up, to compute the mean saturation throughput S for the bus network of Fig. 3 with N terminal LoCs under exclusive access policy we follow these steps: 1) fix the volume v of the payload droplets, 2) dimension the network according to the theoretical background seen in the previous sections; 3) reckon the time b_n for each destination $n = 1, \ldots, N$; 4) compute S as in (27).

We applied this procedure to a system with the parameters reported in the rightmost column of Tab. I, obtaining the throughput shown in Fig. 5. The square markers refer to the throughput obtained with payload droplet of same length ℓ_N as the longest header droplet, while the circle markers report the throughput with payload droplets of halved length.

TABLE I
SYSTEM PARAMETERS SETTING

Symbol	Meaning	Setting
w	channels width	150 μm
h	channels height	50 μm
μ_c	continuous phase viscosity	1.002 mPa s
μ_d	dispersed phase viscosity	145.5 mPa s
α	design parameter	5
β	design parameter	$1/2$
L	Secondary branches distance in bus network	5.4 mm
χ	dimensionless parameter	0.187
σ	interfacial tension coefficient	0.046 N/m

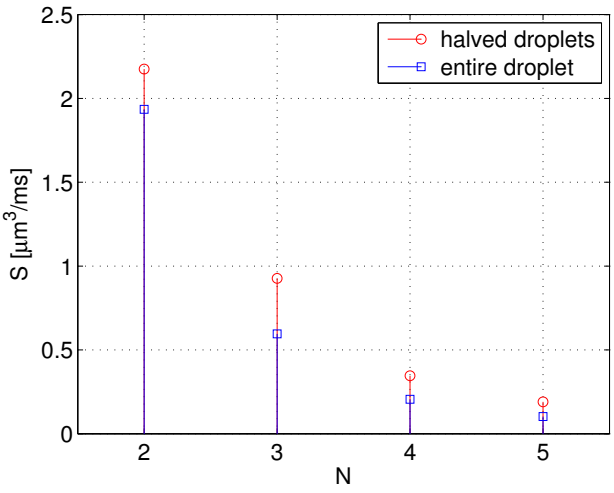

Fig. 5. Comparison of the mean throughput obtained forwarding a single payload droplet or two halved drops.

As expected, the mean throughput quickly decreases as the number N of terminal LoCs increases, because the larger N, the longer the outlets and, consequently, the larger the droplet crossing time. Furthermore, the exclusive access policy prevents the transmission of new droplets until previous ones have exited the system, thus penalizing networks with longer delivery time. Finally, every new LoC added to the bus requires correspondingly longer header droplets, as for (18), so that the maximum input speed u^* decreases according to (28).

A somehow unexpected result, instead, is that smaller droplets achieve higher throughput, which is counterintuitive considering that we need twice the number of header-payload droplets to deliver the same volume of dispersed fluid to the destination. The reason of this performance gain is that smaller payload droplets make it possible to increase u^*, while reducing the resistance of the crossed channels and, hence, the crossing time. However, these advantages are quickly absorbed by the overhead due to multiple transmissions when the size of the payload droplets decreases too much, because the input velocity of the system gets limited by the length of the header droplets.

V. CONCLUSIONS

In this paper we illustrated the main concepts of droplet based microfluidic and proposed simplified mathematical models to effectively describe them. In this way, we were able to implement complex routing functions in LoC context by using totally passive techniques based on microfluidic physical laws. As a proof of concept, we applied the models to the design of a pure hydrodynamic network with bus topology, for which we derive the throughput, in terms of average volume of dispersed flow delivered to the intended LoC in the unit time, and draw a number of considerations.

Clearly, several research challenges remain open: design of more sophisticated scheduling algorithm, investigation of other network topologies, extension of the mathematical models for basic microfluidic elements, just to mention a few.

REFERENCES

[1] P. Tabeling, "Introduction to Microfluidics". Oxford Univ. Press, 2005.
[2] S. Y. Teh, R. Lin, L. H. Hung and P. L. Abraham, "Droplet microfluidics", *Lab Chip*, 8(2), pp.198-220, 2008.
[3] E. De Leo, L. Galluccio, A. Lombardo, G. Morabito, "On the feasibility of using microfluidic technologies for communications in Labs-on-a-Chip", Proc. of IEEE ICC 2012.
[4] ——, "Networked Labs-on-a-Chip (NLoC): Introducing networking technologies in microfluidic systems", *Nano. Com. Net.*, Vol. 3, Issue 4, pp.217-228, Dec. 2012.
[5] D. R. Link *et al.*, "Electric control of droplets in microfluidic devices", *Angewandte Chemie Int. Ed.*, 45(16), pp. 2556-2560, 2006.
[6] D. A. Sessoms *et al.*, "Droplet motion in microfluidic networks: Hydrodynamic interactions and pressure-drop measurements", *Phys. Rev. E.*, 80, 2009.
[7] M. J. Fuerstman, P. Garstecki, G. M. Whitesides, "Coding/decoding and reversibility of droplet trains in microuidic networks", *Science*, 315(5813), pp.828-831, 2007.
[8] M. Prakash, N. Gershenfeld, "Microuidic bubble logic", *Science*, 315(5813), pp.832-835, 2007.
[9] C. N. Baroud, F. Gallaire, R. Dangla, "Dynamics of microfluidic droplets", *Lab Chip*, 10, pp.2032-2045, 2010.
[10] T. Thorsen *et al.*, "Dynamic pattern formation in a vesicle-generating microfluidic device", *Phys. Rev. Lett.*, 86, pp.4163-4166, 2001.
[11] P. Garstecki *et al.*, "Formation of droplets and bubbles in a microfluidic T-junction - scaling and mechanism of break-up", *Lab Chip*, 6, pp.437-446, 2006.
[12] A. Carlson, M. Do-Quang and G. Amberg, "Droplet dynamics in a bifurcating channel", *Int. J. Multiphase Flow*, 36, pp.397-405, 2010.
[13] D. R. Link *et al.*, "Geometrically mediated breakup of drops in microfluidic devices", *Phys. Rev. Lett.*, 92, 2004.
[14] A. M. Leshansky and L. M. Pismen, "Breakup of drops in a microfluidic T junction", *Phys. Fluids*, 21, 2009.
[15] G. F. Christopher *et al.*, "Coalescence and splitting of confined droplets at microfluidic junctions", *Lab Chip*, 9(8), pp.1102-1109, 2009.
[16] M. C. Jullien *et al.*, "Droplet breakup in microfluidic T-junctions at small capillary numbers", *Phys. Fluids*, 21, 2009.

[17] S. Afkhami, A. M. Leshansky, Y. Renardy, “Numerical investigation of elongated drops in a microfluidic T-junction”, *Phys. Fluids*, 23, 2011.
[18] W. O. Kwang *et al.*, “Design of pressure-driven microfluidic networks using electric circuit analogy”, *Lab Chip*, 12, pp.515-545, 2012.
[19] A. Ajdari, “Steady flows in networks of microfluidic channels: building on the analogy with electrical circuits,” *Comptes Rendus Phys.*, 5(5), pp.539-546, 2004.